Muetterties' more recent flow system is in marked contrast to the experimental data presented here. Whereas our flow reactor yields results complementary to our recycle system, showing an increase in chloromethane production and more complete conversion of CO to volatile products, the Muetterties flow system shows quite different chemistry. The latter reaction is approximately four times faster than both our catalytic systems and the initially reported static reaction and produces higher hydrocarbon products, predominantly propane (17%), isobutane (54%), and pentanes (17%), *without alkyl halides*. Muetterties rationalizes the discrepancy in chain length as arising from cracking reactions of the heavier alkanes in the static reactor. This runs contrary to literature reports[31,57] and our observations, which show isomerization as the major reaction of C_4–C_6 hydrocarbons, accompanied by minor cracking but very little methane or ethane production. In addition, there is a dramatic difference in the initial stages of the two reactions, one showing a very active period representing tens of turnovers to three- and four-carbon products, while ours produces only a stoichiometric amount of alkanes, primarily methane.

Attempts to duplicate these recently reported experimental results in our laboratory have been unsuccessful. (Changes in catalyst preparation, catalyst pretreatment, catalyst concentration, reactant purification procedures, flow rates, and temperature all lead to results similar to those described herein.) The two systems are so dramatically different that we must conclude that they represent two different active catalysts, albeit from the same precatalyst under similar conditions. Thus, the Muetterties flow reaction remains a novel and intriguing syngas transformation. Since we have been unable to reproduce this catalytic system, we have confined speculation to our own results, which appear to be both self-consistent and consistent with the homogeneous literature.

Finally it should be evident that a catalytic CO–H_2 process which consumes $AlCl_3$ has no technological significance. In spite of this, the present study may have some heuristic merit.

Acknowledgment. We wish to acknowledge the assistance of Prof. Michel Boudart (Department of Chemical Engineering, Stanford University) and Dr. Ralph Dalla Betta (Catalytica Associates, Santa Clara, CA) as well as the analytical aid of Dr. P. Jones (University of the Pacific, Stockton, CA, for H_2–HD–D_2 mass spectroscopy) and Catalytica Associates (GC/MS analyses). Financial support from the National Science Foundation (Grant CHE78-09443) is also gratefully acknowledged.

Registry No. NaCl, 7647-14-5; CO, 630-08-0; tetrairidium dodecacarbonyl, 18827-81-1; methane, 74-82-8; ethane, 74-84-0; methyl chloride, 74-87-3; methanol, 67-56-1; aluminum chloride, 7446-70-0.

(57) Ohtsuka, Y.; Tamai, Y. *J. Catal.* **1981**, *67*, 316-323.

Kinetics and Mechanism of the Formation of Nitrosoalkane Complexes by Migratory Insertion of Coordinated Nitric Oxide into Cobalt–Carbon Bonds

Wayne P. Weiner and Robert G. Bergman*

Contribution from the Department of Chemistry, University of California, Berkeley, California 94720. *Received September 20, 1982*

Abstract: Treatment of $[CpCoNO]_2$ with Na/Hg in Et_2O results in the formation of the salt $Na^+[CpCoNO]^-$ (**4**). Reaction of **4** with CH_3I in THF at −40 °C gives the methyl nitrosyl complex **5a**, which decomposes at higher temperatures in the absence of phosphines. When solutions of **5a** are warmed above −40 °C in the presence of at least 1 equiv of PPh_3, clean conversion to a product formed by NO migratory insertion, $CpCo(RNO)PPh_3$ (R = CH_3, **6a**), is observed. In a similar manner, treatment of **4** in the presence of PPh_3 with the appropriate alkylating agents afforded the series of nitrosoalkane complexes **6**, where R = Et, *i*-Pr, and *p*-methylbenzyl. All of these complexes were isolated and fully characterized. One method of removing the organic ligand from the nitrosoalkane complexes was demonstrated by treating **6d** with $LiAlH_4$, which gave a high yield of *p*-methylbenzylamine. The bonding in these complexes, in particular the η^1-nitrosoalkane ligand, was established by an X-ray diffraction analysis of **6b** (R = Et). Labeling studies showed that the insertion is an intramolecular process and that β elimination, when possible, does not compete with the NO insertion. Kinetic studies indicated that the rate of reaction ($k = 1.6 \times 10^{-3}$ s^{-1} at 18 °C) of **5a** to **6a** does not vary as a function of $[PPh_3]$. This result requires the rate-determining formation of an intermediate, which in the phosphine concentration range studied (0.05–0.20 M), is always trapped by a ligand faster than it can return to starting material. One possible formulation of this intermediate is the coordinatively unsaturated complex $CpCo(CH_3NO)$ (**7**). When **5a** is generated in the presence of PEt_3, a new complex is formed, which was identified on the basis of spectroscopic data as $CpCo(NO)(CH_3)(PEt_3)$ (**8a**), where the coordinated NO group has adopted a bent geometry. Complex **8a** undergoes insertion to give the nitrosomethane complex **6e**. Kinetic studies showed that the reaction of **8a** to **6e** is not a simple unimolecular process but that **8a** must undergo dissociation of the PEt_3 ligand to regenerate **5a** before the migratory insertion can occur. This result is analyzed in terms of the relative binding energies of PEt_3 to the nitrosyl methyl complex **5a** and to the transition state leading to NO insertion, **5‡**. A mechanism consistent with the kinetic and labeling data is proposed and discussed.

Migratory insertion of CO into transition-metal–carbon bonds (eq 1) is one of the most ubiquitous and well-studied reactions in organotransition-metal chemistry.[1] In addition to its fundamental importance, CO migratory insertion is a critical step in many important carbon–carbon bond forming processes involving homogeneous transition-metal catalysts.[2] In contrast, migratory insertion of NO into metal–carbon bonds (eq 2) is much less common and in most cases has only been inferred as one step in a more complicated overall transformation.

$$R—M(CO) + L \rightarrow R—C(=O)—M(L) \quad (1)$$

$$R—M(NO) + L \rightarrow R—N(=O)—M(L) \quad (2)$$

(1) (a) Calderazzo, F. *Angew. Chem., Int. Ed. Eng.* **1977**, *16*, 299-311. (b) Kuhlman, E. J.; Alexander, J. J. *Coord. Chem. Rev.* **1977**, *33*, 195-225.

(2) Parshall, G. W. "Homogeneous Catalysis"; Wiley: New York, 1980.

0002-7863/83/1505-3922$01.50/0

Scheme I

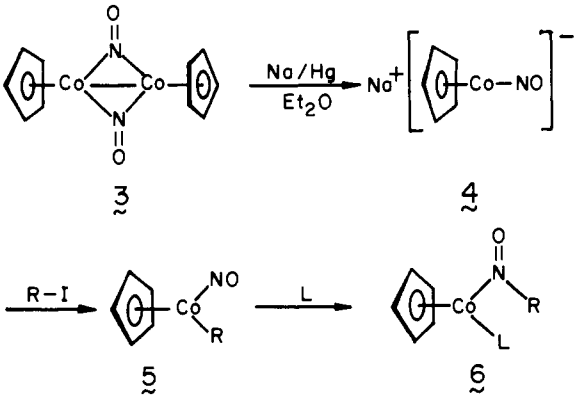

a) R = CH_3, L = PPh_3

b) R = CH_2CH_3, L = PPh_3

c) R = $CH(CH_3)_2$, L = PPh_3

d) R = p-$CH_2(C_6H_4)CH_3$, L = PPh_3

e) R = CH_3, L = PEt_3

One such example was reported by Wailes, Weigold, and Bell,[3] where the Zr complex **1** was isolated from the reaction of dicyclopentadienyldimethylzirconium with NO gas. A similar product with respect to the bonding of the ligand formed by NO insertion, **2**, has been characterized by Wilkinson[4] in the reaction of NO gas with hexamethyltungsten. Another case in which NO insertion is likely to have occurred is in work by Eisenberg, where the formation of 3-oximinopropene is observed from the reaction of $M(NO)(\eta^3\text{-}C_3H_5)(PPh_3)_2$ (M = Rh, Ir) with CO gas.[5]

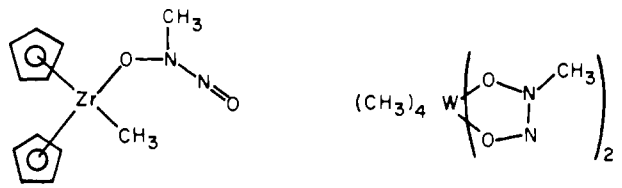

Although spectroscopic evidence for NO insertion has been obtained by IR and ^1H NMR spectroscopy,[6] this study represents the first fully documented direct observation of the conversion of a well-defined alkyl nitrosyl complex into a simple nitrosoalkane complex, with a complete characterization of the latter. The synthesis of the starting alkyl nitrosyl complex involved the generation, isolation, and alkylation of a low-valent metal nitrosyl anion. In addition, the results of the first mechanistic study of the NO insertion reaction are reported.[7]

Results and Discussion

Preparation and Conversion of $Na^+[CpCoNO]^-$ into Nitrosoalkane Complexes. Our system is outlined in Scheme I. After several trial experiments, it was found possible to successfully reduce Brunner's[8a,b] dimer (**3**) to the sodium salt $Na^+[CpCoNO]^-$ (**4**) by carrying out the reduction in diethyl ether. The salt precipitates from the reaction solution as a pink pyrophoric solid in 85–90% yield. The ^1H NMR spectrum of **4** in THF-d_8 exhibits a cyclopentadienyl resonance at δ 4.1. The salt shows two IR absorptions in the M–NO region in THF (1560, 1530 cm^{-1}) but only one (1570 cm^{-1}) in acetonitrile. Presumably this reflects the absence of ion pairing in the more polar solvent. The sodium salt can be metathesized with $[(PPh_3)_2N]^+Cl^-$ (PPNCl) to give PPN-**4**, which can be recrystallized from CH_3CN/Et_2O to form moderately air-stable red crystals.[8c]

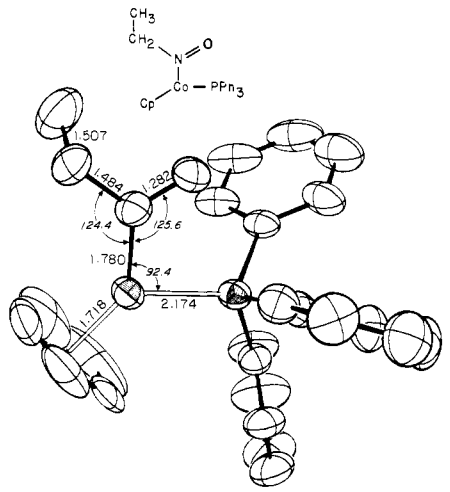

Figure 1. ORTEP drawing of **6b** including important bond distances and angles.

Addition of 1 equiv of CH_3I to a THF solution of **4** at room temperature led rapidly to decomposition products. However, monitoring the reaction by ^1H NMR spectroscopy at −40 °C showed that alkylation occurred immediately leading to a new complex which exhibited a higher frequency M–NO absorption at 1780 cm^{-1} and two singlets in the ^1H NMR spectrum (THF-d_8), one at δ 5.15 (5 H) and the other at δ 1.93 (3 H). On the basis of these data we assign to this material the structure of the methyl nitrosyl complex **5a**. It is stable in solution below −30 °C but decomposes rapidly upon attempted isolation or warming above this temperature in the absence of phosphines. When the solution of **5a** was warmed to room temperature in the presence of 1 equiv of PPh_3, the complex was transformed into a new material having an IR absorption at 1310 cm^{-1} and ^1H NMR resonances at δ 4.52 (s, 5 H) and 2.63 (d, 3 H, J = 2.6 Hz), consistent with its formulation as the NO insertion product **6a**. Similar observations were made in the reaction of nitrosyl anion **4** with ethyl and isopropyl iodide in the presence of PPh_3, to form the corresponding nitrosoalkane complexes **6b–c**. The bonding in **6b** (and presumably in **6a,c,d**) was confirmed by an X-ray diffraction analysis.[7] In particular, the η^1 bonding of the nitrosoethane ligand to the cobalt atom was clearly shown. An ORTEP drawing of **6b**, along with important bond lengths and angles, is given in Figure 1.

Treatment of anion **4** with *p*-methylbenzyl bromide in the absence of phosphines gave immediate reaction to form the benzyl nitrosyl complex **5d**, with a strong NO absorbance at 1790 cm^{-1}. The ^1H NMR spectrum of **5d** in C_6D_6 exhibits aromatic resonances at δ 7.10 (m, 4 H) and singlets at δ 4.57 (2 H), 4.44 (5 H), and 2.09 (3 H). Solutions (ca. 0.2 M in THF) of this complex have a half-life at room temperture of about 40 min,[9] and it could not be isolated in analytically pure form. In the presence of PPh_3, **5d** is converted into the inserted product **6d**. Treatment of **6d** with

(3) Wailes, P. C.; Weigold, H.; Bell, A. P. *J. Organomet. Chem.* **1972**, *34*, 155–164.

(4) Shortland, A. J.; Wilkinson, G. *J. Chem. Soc., Dalton Trans.* **1973**, 873–876. See also: Middleton, A. R.; Wilkinson, G. *Ibid.* **1981**, 1898–1905.

(5) (a) Schoonover, M. W.; Baker, E. C.; Eisenberg, R. *J. Am. Chem. Soc.* **1979**, *101*, 1880–1882. See also: (b) Clement, R. A.; Klabunde, U.; Parshall, G. W. *J. Mol. Catal.* **1978**, *4*, 87–94.

(6) (a) Klein, H.; Karsch, H. *Chem. Ber.* **1976**, *109*, 1453–1464. (b) Middleton, A. R.; Wilkinson, G. *J. Chem. Soc., Dalton Trans.* **1980**, 1888–1892.

(7) Preliminary results have been reported earlier: Weiner, W. P.; White, M. A.; Bergman, R. G. *J. Am. Chem. Soc.*, **1981**, *103*, 3612–3614. Details of the crystallographic study are included in the supplementary information provided with this communication.

(8) (a) Brunner, H. *J. Organomet. Chem.* **1968**, *12*, 517–522. (b) Brunner, H.; Wachsmann, H. *Ibid.* **1968**, *15*, 409–421. (c) **Note Added in Proof**: An X-ray structure of the MeCp analogue of PPN-**4** has been completed and will be reported at a later date; it shows a Co–N–O angle very close to 180°.

(9) Qualitatively, the relative rates of insertion decrease in the order Et, isopropyl > Me > benzyl, a trend which has also been observed for CO insertion. See: (a) Cotton, J. D.; Crisp, G. T.; Lati, F. *Inorg. Chim. Acta* **1981**, *47*, 171–175. (b) Cotton, J. D.; Crisp, G. T.; Daly, V. A. *Ibid.* **1981**, *47*, 165–169.

Scheme II

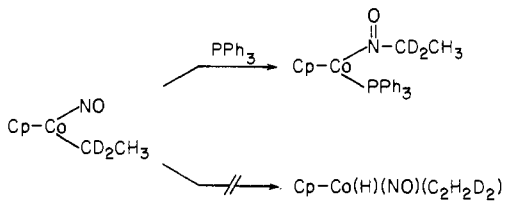

Scheme III

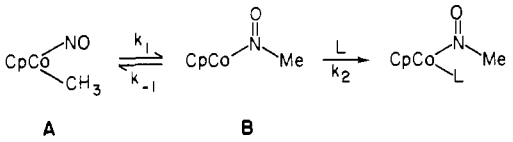

$LiAlH_4$ in THF affords a high yield (90%) of *p*-methylbenzylamine, which was isolated from the reaction as its HCl salt. Presumably this procedure could be extended to nitrosoalkane complexes **6a–c**.

Preliminary experiments showed that the use of trifluoromethylsulfonates as alkylating agents resulted in reduced yields of the final nitrosoalkane products. Although methyl *p*-toluenesulfonate and methyl iodide displayed comparable reactivity toward anion **4**, ethyl and isopropyl *p*-toluenesulfonates did not react with **4** at room temperature. *p*-Methylbenzyl bromide and the corresponding *p*-toluenesulfonate were equally effective in the alkylation of **4**, and both gave cleaner reactions than the analogous iodides.

The nitrosoalkane complexes are unstable toward column chromatography, and were best purified from the crude reaction mixtures by recrystallization from toluene (or CH_2Cl_2)/pentane at −40 °C. The dark crystals that formed were isolated in yields that ranged from good (80% for nitrosomethane complex **6a**) to poor (15% for *p*-methylbenzyl complex **6d**). Control experiments by ^1H NMR spectroscopy showed that the actual formation of the complexes **6a,b,d** occurred in good yield (70–95%) but that isopropyl complex **6c** was formed in only 30% yield. The complexes are moderately air stable as solids at room temperature. They can be stored as solids under nitrogen indefinitely at −40 °C but begin to decompose in solution after 12 h at room temperature.

No evidence for the formation of free or bound alkenes during the transformation of **5b–c** to **6b–c** was observed during ^1H NMR monitoring of these reactions. This indicates that β elimination, a common decomposition route for alkyl complexes,[10] does not compete with the NO insertion. The absence of a reversible β elimination process is supported by the observation that the transformation of $CpCo(NO)(CD_2CH_3)$ to the corresponding insertion adduct gave no interchange of hydrogen atoms between the α and β positions (Scheme II).

Mechanism of NO Migratory Insertion in the Presence of PPh_3. One possible pathway for the NO insertion reaction involves reversible, rate-determining alkyl migration to form an unsaturated intermediate (B) which might be trapped by a ligand L (Scheme III). According to this mechanism, the reaction rate is given by eq 3. If at high [L], $k_2[L] \gg k_{-1}$, the pseudo-first-order rate constant k_{obsd} is equal to k_1.

$$\text{rate} = \frac{k_1 k_2[L]}{k_{-1} + k_2[L]}[A] = k_{obsd}[A] \qquad (3)$$

The change in k_{obsd} for the transformation of methyl complex **5a** to nitrosomethyl complex **6a** as a function of $[PPh_3]$ was conveniently followed at 18 °C by UV/vis spectroscopy. With use of syringe techniques, CH_3I was added under an argon flow to a serum-stoppered cuvette at 18 °C containing a THF solution of known concentrations of **4** and PPh_3.[11] In this manner, the reaction was initiated by the in situ formation of **5a**.

Table I. Rate Constants for Conversion of 5a to 6a in the Presence of Varying Concentrations of PPh_3 at 18 ± 0.5 °C

run	10^4[5a] mol/L	10^3[PPh_3], mol/L	$10^3 k_{obsd}$, s^{-1}
1	9.60	5.0	1.47
2	8.59	10.0	1.49
3	4.86	20.0	1.54
4a	8.13	50.0	1.61
4b	8.13	50.0	1.60
4c	8.13	50.0	1.68
5	8.59	100	1.59
6a	8.36	150	1.61
6b	8.36	150	1.67
7	5.08	200	1.69

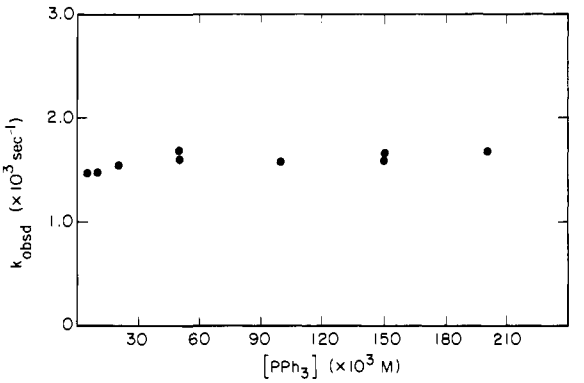

Figure 2. Plot of k_{obsd} vs. $[PPh_3]$ for the conversion of **5a** to **6a**.

Scheme IV

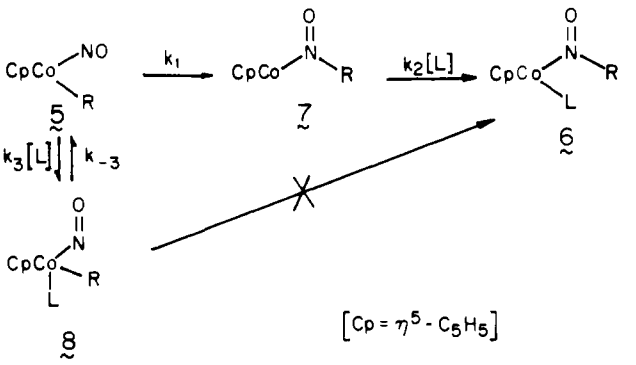

The absorbance change at λ 412 nm was recorded as a function of time, and from this information, the value of k_{obsd} for a given $[PPh_3]$ was derived. In each of the runs listed in Table I, the disappearance of **5a** and the formation of **6a** followed good pseudo-first-order kinetics. A plot of the k_{obsd} values vs. $[PPh_3]$ (Figure 2)shows that a 40-fold increase in $[PPh_3]$ produces only a very weak response in k_{obsd}. This requires the rate-determining formation of an intermediate which, in the concentration range studied, is always trapped by ligand faster than it can return to starting material. It seems most reasonable that this intermediate is the coordinatively unsaturated[12] (or THF-solvated) complex **7** (Scheme IV). Under these conditions, $k_{obsd} = k_1$, the unimolecular rate constant for NO migratory insertion.

Insertion in the Presence of PEt_3. When methyl nitrosyl complex **5a** is generated in the presence of PEt_3 at −60 °C, its behavior is initially different from that observed with PPh_3. The species first observed by ^1H NMR spectroscopy in THF-d_8 solution

(10) (a) Schrock, R. R.; Parshall, G. W. *Chem. Rev.* **1976**, *76*, 243–268. (b) Davidson, P. J.; Lappert, M. F.; Pearce, R. *Ibid.* **1976**, *76*, 219–242.

(11) The extent of the reaction of PPh_3 with MeI during the course of the kinetic run is insignificant. See: Pearson, R. G.; Figdore, P. E. *J. Am. Chem. Soc.* **1980**, *102*, 1541–1547.

(12) A coordinatively saturated η^2-bound nitrosoalkane ligand is also a possible formulation of the intermediate **7**. A recent calculation carried out by P. Hoffmann and M. Padmanabhan predicts that the η^2- and bent η^1-bonded structure have comparable energies (manuscript submitted for publication).

Table II. Rate Constants for Conversion of 8a to 6e in the Presence of Varying Concentrations of PEt_3 at 28 ± 0.5 °C

run	10^2[5a], mol/L	10^2[PEt_3], mol/L	$10^4 k_{obsd}$, s^{-1}	$10^{-3} \times (1/k_{obsd})$, s
1	0.835	2.80	8.18	1.22
2	1.67	7.54	4.69	2.13
3	3.30	16.6	1.87	5.35
4	5.60	10.0	2.37	4.22
5	6.00	30.0	1.10	9.09
6	9.20	21.1	1.73	5.78
7	19.0	40.7	0.936	10.7

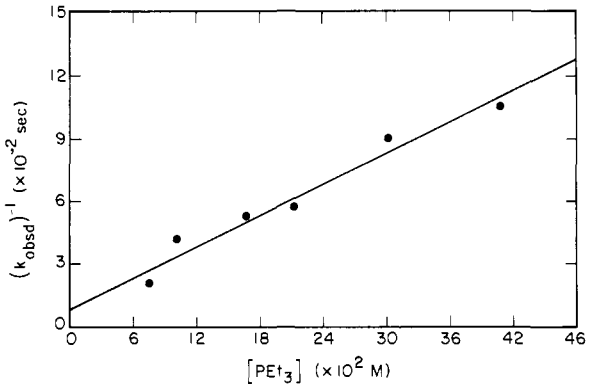

Figure 3. Plot of $1/k_{obsd}$ vs. [PEt_3] for the conversion of **8a** to **6e**.

displays a cyclopentadienyl resonance at δ 5.5 (s, 5 H) and a new methyl resonance at δ −0.07 (d, 3 H, J = 5.2 Hz) in addition to bound PEt_3 resonances. The IR spectrum of this species shows a single strong low-frequency M–NO stretch at 1530 cm^{-1}. The complex which is most consistent with these data is a phosphine addition product **8a** (Scheme IV), in which bending of the nitrosyl group accommodates the new ligand at the cobalt center. Presumably **8a** is formed by direct attack of PEt_3 on **5a**; the rate of this reaction is too rapid at −60 °C to be measured by ^1H NMR spectroscopy. When the mixture is warmed to room temperature, adduct **8a** is converted quantitatively to a complex which displays in the ^1H NMR spectrum (in addition to the resonances of bound PEt_3) a cyclopentadienyl resonance at δ 4.62 (s, 5 H) and a methyl resonance at δ 2.39 (d, 3 H, J = 3 Hz) and has an IR absorption in the M–NO region at 1315 cm^{-1}. Comparison of these spectral data with those of **6a** allow identification of this new complex as the NO insertion product $CpCo(CH_3NO)(PEt_3)$ (**6e**).

If the formation of **6e** from **8a** occurs directly, then k_{obsd} for the transformation should be independent of added [PEt_3]. If, on the other hand, **6e** is formed by dissociation of PEt_3 from adduct **8a** to regenerate methyl nitrosyl complex **5a**, phosphine inhibition should be observed. In order to resolve this question, the bent nitrosyl adduct **8a** was generated at −50 °C in THF-d_8 in the probe of an NMR spectrometer, in tubes containing varying excess concentrations of PEt_3. By monitoring the changes of the cyclopentadienyl resonances of **8a** and **6e** at 28 °C against a ferrocene internal standard, k_{obsd} for the conversion of **8a** to **6e** was determined as a function of [PEt_3]. As before, good first-order kinetics were observed. The data from this study are given in Table II, and show a *strong rate inhibition with increasing* [PEt_3]. These results demonstrate that the conversion of **8a** to **6e** is not a simple unimolecular process. They suggest strongly that *complex* **8a** *does not undergo NO insertion to give* **6e** *directly*; rather, reaction involves initial dissociation of PEt_3 from **8a** as shown in Scheme IV. According to this mechanism, the rate and k_{obsd} for the insertion are given by eq 4 and 5, where the rate constants are

$$\text{rate} = \frac{k_{-3}k_1}{k_3[\text{L}] + k_1}[\mathbf{8}] \tag{4}$$

$$\frac{1}{k_{obsd}} = \frac{k_3[\text{L}]}{k_1 k_{-3}} + \frac{1}{k_{-3}} \tag{5}$$

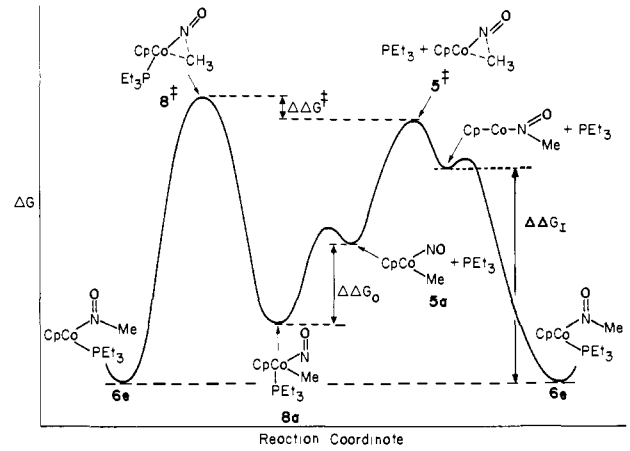

Figure 4. Proposed free energy vs. reaction coordinate diagram for the NO migratory insertion reaction (a standard state of 1 mol L^{-1} for the phosphine concentration is assumed).

those defined in Scheme IV. In principle, from the slope and intercept of the plot of $1/k_{obsd}$ vs. [L] shown in Figure 3, one can calculate both k_{-3} and the rate constant ratio k_3/k_1. Unfortunately, the scatter in the data is great enough that significant error develops in the attempt to calculate the low intercept $1/k_{-3}$. From a standard least-squares analysis we obtain $k_{-3} = (1.2 \pm 0.6) \times 10^{-3}$ s^{-1} and $[k_3/k_1] = 31 \pm 16$ M^{-1}. These values are obviously not very precise, but one at least obtains from them an idea of the order of magnitude of the rates involved in the mechanism. Thus, at 1 M [PEt_3], the formation of **8a** from **5a** appears to be somewhat faster than the insertion step, and at higher phosphine concentrations it is reasonable that the linear nitrosyl **5a** is essentially irreversibly trapped before it can undergo insertion.[13] Under these conditions dissociation of PEt_3 (k_{-3}) from the bent nitrosyl adduct **8a** becomes the rate-determining step of the reaction.

It is surprising that the adduct **8a**, formed by the entry of triethylphosphine into the cobalt coordination sphere and bending the NO group in **5a**, does not provide a facile pathway leading to the NO migratory insertion product **6e**. It seemed likely to us that entry of the phosphine ligand might provide a "push" which would drive the conversion of **8a** to the insertion product **6e**. In the analogous migratory insertions of CO, there is good evidence for assistance by solvent molecules and phosphine ligands in the migratory insertion process.[14] However, in the nitric oxide case phosphine is clearly not involved in the migratory insertion transition state.

We believe it is useful to discuss this result employing the idea of ground- and transition-state binding energies, a concept which has become common in comparing catalyzed and uncatalyzed pathways for reactions mediated by enzymes.[15] In order to do this more clearly, we refer to the free energy diagram illustrated in Figure 4. The curve in the right half of this diagram represents the proposed pathway for migratory insertion in nitrosyl alkyl complex **5a**, which leads to nitrosoalkane complex **6e**. As our kinetic study requires, the migratory insertion step is rate determining, and coordination of phosphine occurs in a rapid second step, over a barrier lower than that for deinsertion. The left-hand side of the diagram illustrates the (undetected and therefore relatively high barrier) pathway for the *direct* conversion of triethylphosphine adduct **8a**, which also leads to insertion product **6e**.

Let us use **5**‡ to represent the first (rate-determining) insertion transition state formed from **5a** and **8**‡ to represent the transition

(13) A similar overall mechanism has been observed for a CO insertion reaction. See: Heck, R. F.; Garrou, P. E. *J. Am. Chem. Soc.* **1976**, *98*, 4115–4127.

(14) Wax, M. J.; Bergman, R. G. *J. Am. Chem. Soc.* **1981**, *103*, 7028–7030.

(15) Jencks, W. P. "Catalysis in Chemistry and Enzymology"; McGraw-Hill: New York, 1969.

state leading directly from adduct **8a** to **6e**. We now wish to consider the energy required to bind PEt_3 to three different species on this reaction coordinate: the alkylnitrosyl complex **5a**, the (presumably) coordinatively unsaturated intermediate CpCo(MeNO), and the transition state **5‡** leading to this intermediate. The gap between starting complexes **5a** and **8a**, labeled $\Delta\Delta G_0$ on the diagram, represents the binding energy for the addition of PEt_3 to **5a**, i.e. the free energy change for the equilibrium shown in eq 6. In the PEt_3 case (illustrated) this binding energy is large and positive (i.e., the reaction as shown in eq 6 has a large equilibrium constant and negative free energy); in the PPh_3 case it is small. The gap between CpCo(MeNO) and **6e**, labeled $\Delta\Delta G_1$, is the energy released on attaching phosphine to the open coordination site on this intermediate (eq 7). As might be expected, this is a very exoergic reaction (large negative free energy) for both PPh_3 and PEt_3. As illustrated in Figure 4, the two first *transition states* also differ by the presence or absence of a phosphine ligand coordinated to the metal center. Thus the difference in free energies between **5‡** and **8‡** can also be thought of as a binding energy, in this case between **5‡** and PEt_3 (eq 8).

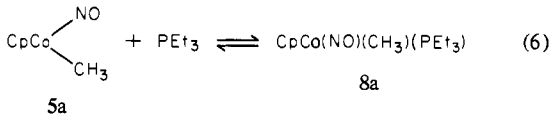

(6)

$$CpCo(CH_3NO) + PEt_3 \rightleftharpoons \underset{\textbf{6e}}{CpCo(CH_3NO)PEt_3} \quad (7)$$

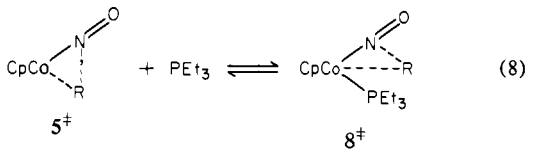

(8)

As may be seen from the diagram, *not only does the transition state coordinate phosphine very weakly, but the binding energy* $\Delta\Delta G^{\ddagger}$ *is actually negative* (i.e., at $[PEt_3] = 1$ mol L^{-1}, the adduct **8‡** would be largely dissociated to **5‡** and free PEt_3). This conclusion is required by the fact that conversion of the adduct **8a** to insertion product **6e** over the direct pathway involving **8‡** is slower than reaction via the path involving initial dissociation of PEt_3; this places the phosphine-bound transition-state **8‡** at a higher free energy than the dissociated transition state **5‡**.

This is an especially perplexing result when considered in comparison with the phosphine affinities of the species connected directly to **5‡**. Both the alkyl complex **5a** and its rearranged isomer CpCo(MeNO) have strong affinities for PEt_3, but in **5‡** (which must have a structure somewhere in between them) this affinity for phosphine is greatly attenuated. We do not understand the physical basis for this curious trend, but we believe this type of analysis suggests a useful framework in which to formulate more extensive theoretical investigations of such relative reactivities.

Intramolecularity of the Insertion Reaction. In order to determine whether intermolecular processes intervene in the NO insertion, a THF-d_8 solution of $MeCpCo(NO)(CH_3)$ with 95% ^{13}C enrichment of the metal-bound methyl ligand was prepared and mixed at −78 °C with a THF-d_8 solution of **5a**, both solutions containing 1 equiv of PPh_3. The solution was then transferred into an NMR tube at −196 °C. The $^{13}C\{^1H\}$ NMR spectrum of the reaction solution at −60 °C showed no enhancement of the metal-bound methyl resonance of **5a**. The sample was then warmed to room temperature; after 40 min, the $^{13}C\{^1H\}$ NMR spectrum of the reaction mixture revealed no significant isotopic enhancement (<10%) of the methyl group in the nitrosomethane ligand of **6a**. The absence of exchange of the ^{13}C-enriched methyl group during the course of the reaction confirms that the NO insertion is an intramolecular process, as shown in Scheme V, involving no transfer of alkyl groups between methyl centers.[16]

Scheme V

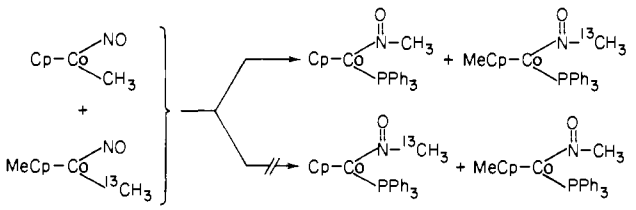

Scheme VI

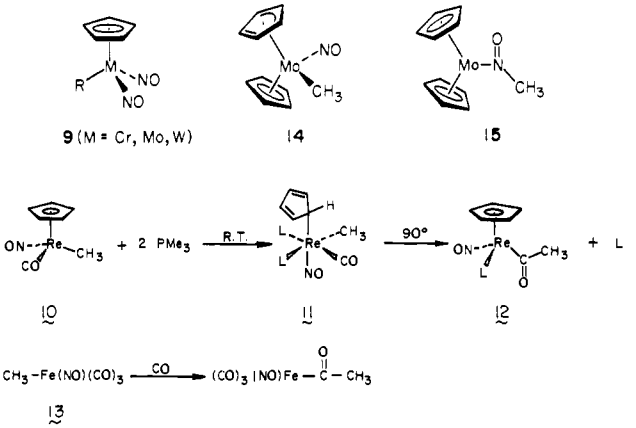

Summary and Conclusions

The treatment of cobalt nitrosyl anion **4** at low temperature with various alkylating agents leads to the formation of a series of alkyl nitrosyl complexes **5a–d**. At room temperature in the presence of PPh_3, these complexes undergo an NO migratory insertion process to form the corresponding series of nitrosoalkane complexes **6a–d**, which can be isolated and characterized. It was demonstrated in one case (**6d**) that the nitrosoalkane ligand can be reductively removed as the corresponding amine by treatment of the complex with $LiAlH_4$. The bonding in these complexes was confirmed by an X-ray diffraction study of nitrosoethane complex **6b**. The results of labeling studies revealed that the insertion is intramolecular and that β elimination does not compete with the insertion process. The k_{obsd} for the transformation of methyl complex **5a** to nitrosomethane complex **6a** does not vary as a function of $[PPh_3]$, and at 18 °C the rate for the methyl migration is on the order of 1.6×10^{-3} s^{-1}. If the nitrosylalkyl complex is generated in the presence of PEt_3, a new phosphine adduct is formed, which we believe has a bent nitrosyl ligand. This complex cannot undergo NO insertion itself but instead must dissociate the phosphine before it rearranges to the final nitrosoalkane complex. A mechanism consistent with our results is shown in Scheme IV.

To our knowledge this is the first nitric oxide migratory insertion system which has been amenable to a kinetic and mechanistic study. There are some similarities between this reaction and the much more extensively studied CO migratory insertion reaction; for example, both have been established to be intramolecular processes. However, there are also some striking differences. The CO insertion, at least with metals such as molybdenum and manganese, can easily be assisted in the initial migration transition state by dative ligands such as phosphines or coordinating solvents. In contrast, NO insertion does not seem to require such assistance; in fact, strong donor ligands simply tie up the starting alkyl complex, thus repressing the migration reaction. The initial step in CO migratory insertion is very often easily reversible; we detect no such reversibility in our system, and if it exists, the rate constant for the deinsertion reaction must be much slower than that for reaction of the unsaturated alkyl nitroso intermediate with trapping ligand.

Perhaps most perplexing is the fact that in the system described here, as well as those summarized in the introduction to this paper, insertion is rapid, but in several other cases it does not seem to

(16) Bryndza, H. E.; Evitt, E. R.; Bergman, R. G. *J. Am. Chem. Soc.* **1980**, *102*, 4948–4951.

proceed at all. When reaction does occur, it takes other (sometimes quite unusual) courses, rather than adopt the nitric oxide insertion route. Some examples of insertion-resistant systems are illustrated in Scheme VI. Cyclopentadienyl complexes of type **9** have been known for some time,[17] and they do not undergo NO migratory insertion. We have found in independent work[18] that added phosphine does not induce the reaction, but instead deoxygenates one of the NO groups. In the reaction of rhenium complex **10** with excess PMe_3 at room temperature,[19] the product formed by an NO insertion is not observed. The product formed instead is **11**, in which the cyclopentadienyl ring has reduced its hapticity from η^5 to η^1. At higher temperatures, CO insertion occurs to give the acyl product **12**. The implication that CO insertion is generally more facile than NO insertion is supported by the result that reaction of iron complex **13** under CO forms only CO insertion products.[20] It is also interesting to note that complex **14** avoids a 20-electron configuration by "slipping" the Cp ring to an η^3 configuration.[21] In contrast to the behavior of our complexes, neither bending of the NO group nor insertion to give **15** is observed.

We are seeking other examples of systems in which nitric oxide insertion can be observed and carefully studied. It is our hope that this will yield new methods for metal-based carbon–nitrogen bond formation and also help to answer some of the intriguing questions raised by the research reported in this paper.

Experimental Section

General Data. ^1H NMR spectra were recorded on a Varian EM-390 spectrometer or at 250-, 200-, or 180-MHz on spectrometers equipped with Cryomagnets Inc. magnets, Nicolet Model 1180 data collection systems, and multinuclear variable-temperature probes. All high-field instruments were constructed by Mr. Rudi Nunlist in the UC Berkeley NMR laboratory. All ^1H and ^{13}C NMR spectra are recorded in δ units (ppm downfield from tetramethylsilane). The $^{13}C\{^1H\}$ spectra were recorded at 63.067 MHz with a sweep width of ±6329.11 Hz, 30° pulse angle, and a 5-s delay between pulses. IR spectra were recorded on a Perkin-Elmer Model 283 infrared spectrometer with 0.10-mm sodium chloride solution cells. UV/vis spectra (λ 200–800 nm) were recorded on a Hewlett-Packard 8450A UV/vis spectrophotometer equipped with a 8290 M flexible disk drive. Experiments performed in the drybox refer to a Vacuum Atmospheres Model 553-2 Dri-lab under a nitrogen atmosphere with attached M6-40-IH Dri-train and equipped with a −40 °C freezer.

Unless otherwise noted, all reagents were obtained from commercial suppliers without further purification. Tetrahydrofuran (THF), diethyl ether, benzene, toluene, and spectrophotometric grade pentane used as solvents were distilled under nitrogen from Na/benzophenone. Olefin-free hexanes, purchased from Burdick and Jackson, was distilled under nitrogen from *n*-butyllithium. The acetonitrile and CH_2Cl_2 used were distilled under nitrogen from CaH_2 after being refluxed for 24 h, as was deuterated acetonitrile. Deuterated THF and benzene were vacuum transferred from Na/benzophenone. Deuterated Me_2SO was vacuum transferred from 3A sieves. All alkyl halides were obtained from Aldrich except for CH_3CD_2I (Stohler, 99%D) and $^{13}CH_3I$ (Merck, 90%^{13}C). They were throughly degassed before use and stored over a drop of Hg and a small coil of copper wire. *p*-Methylbenzyl bromide was recrystallized from hexanes before use. PPNCl was purchased from Alfa and recrystallized from THF/hexanes. NO gas was obtained from Matheson. Elemental analyses were performed by the Microanalytical Laboratory operated by the College of Chemistry, UCB.

(η^5-MeC_5H_4)Co(CO)$_2$. Following the procedure reported for the synthesis of $CpCo(CO)_2$,[22] 80 mL of freshly distilled $CH_3C_5H_5$ was treated with 78.0 g (0.229 mol) of $Co_2(CO)_8$. The crude red oil obtained was distilled through a 6-in. Vigreaux column at 91 °C (25 mm) to give 30.0 g (0.154 mol) of the dicarbonyl, which was determined to contain 5% $CH_3C_5H_5$ dimer impurity: HRMS calcd for $C_8H_7O_2Co$, M^+ 194.0732, found M^+ 193.9776; IR (hexanes) 2020, 1970 cm^{-1}; ^1H NMR (C_6D_6) δ 1.4 (s, 3 H), 4.4 (m, 4 H).

[CpCoNO]$_2$ (3). The procedure of Brunner[8] was employed with the following modifications. A 300-mL three-neck round-bottom flask was fitted with a magnetic stir bar, a vacuum stopcock attached to an oil bubbler, and a three-way gas inlet tube which extended deep enough into the flask to allow gases to be bubbled through a stirred reaction solution. Under a flow of argon, the flask was charged with 30.5 g (169 mmol) of $CpCo(CO)_2$ and 150 mL of CH_2Cl_2, which was deoxygenated beforehand by bubbling argon through the solvent for 15 min. NO gas was then allowed to bubble slowly through the reaction solution. The red solution began to darken immediately and continued to turn black over the course of the reaction. The consumption of $CpCo(CO)_2$ was conveniently monitored by TLC (SiO_2, 3/1 pentane/CH_2Cl_2). After 6.5 h, the reaction was stopped and the reaction solution was carefully flushed with argon to remove unreacted NO gas. The solvent was then removed by vacuum transfer, leaving a brown-black powder. The powder was brought into the drybox where it was loaded onto a 600-mL coarse frit packed with SiO_2 (Merck, 70–230 mesh). Under suction, the powder was washed with hexanes to remove unreacted $CpCo(CO)_2$ (ca. 15 g). When the hexane washings were clear, the dimer was collected from the frit by washing with benzene. The solvent was removed by vacuum transfer to yield 6.05 g (19.6 mmol) of product, 47% yield based on reacted $CpCo(CO)_2$: IR (benzene) 1600 (m), 1550 (m) cm^{-1}; ^1H NMR (C_6D_6) δ 4.60 (Cp, s). All spectroscopic data agree with those reported in the literature.[8]

[MeCpCo(NO)]$_2$. With use of the procedure described above, 30.0 g (454 mmol) of $MeCpCo(CO)_2$ was reacted for 4 h (50% consumption of starting material, as determined by IR spectroscopy) with NO gas to give 4.8 g (14.3 mmol; 13% yield) of the dimer: IR (hexanes) 1590 (m), 1540 (m) cm^{-1}; ^1H NMR (C_6D_6) δ 4.48 (m, 4 H), 1.70 (s, 3 H). Anal. Calcd for $C_{12}H_{14}N_2O_2Co$: C, 42.88; H, 4.20; N, 8.34. Found: C, 42.93; H, 4.20; N, 8.26.

Na[CpCoNO] (4). In the drybox, a 500-mL round-bottom flask fitted with an efficient stir bar was charged with 2.0 g (6.4. mmol) of **4** in 200 mL of Et_2O and 8.9 g of 0.5% Na/Hg (19.4 mmol of Na). The reaction mixture was allowed to stir vigorously, and in the course of 20 min, copious amounts of pink precipitate were formed. The precipitate was decanted onto a 300-mL medium frit. The pink residue was then dissolved in a minimum of THF and the solution filtered through a 300-mL fine frit, which removed traces of sodium metal. The deep violet solution was treated with hexanes until no further precipitate was evolved from the solution. The solid was then collected on a 50-mL medium frit and suction dried to yield 1.95 g (9.90 mmol, 85%) of highly pyrophoric **4**. The material was established to be greater than 95% pure by ^1H NMR spectroscopy: IR (THF) 1555 (s), 1525 (s) cm^{-1}; ^1H NMR (THF-d_8) δ 4.15 (Cp, s).

Na[MeCpCoNO]. According to the procedure described above, 1.0 g (2.97 mmol) of $[MeCpCoNO]_2$ in 100 mL of Et_2O with 27.4 g of 1.0% Na/Hg (11.9 mmol of Na) gave 0.975 g (5.08 mmol, 85%) of the sodium salt, which was greater than 95% pure by ^1H NMR spectroscopy: IR (THF) 1540 (s), 1510 (s), 1470 (m) cm^{-1}; ^1H NMR (THF-d_8) δ 4.05 (m, 4 H), 2.17 (s, 3 H).

Metathesis of 4 and Na[MeCpCoNO] with PPNCl. In the drybox, 0.50 g (2.62 mmol) of **3** and 0.752 g (1.31 mmol) of PPNCl in 10 mL of THF were weighed into a 50-mL round-bottom flask fitted with a magnetic stir bar. After being stirred for 3 h, the deep violet solution evolved into an orange suspension. The orange solid was filtered onto a 30-mL fine frit and washed with THF. The solid was then redissolved in CH_3CN and filtered through a 30-mL fine frit. Solvent removal by vacuum transfer left an orange oil, which was recrystallized from 1/1 CH_3CN/Et_2O to give 0.785 g (1.05 mmol) of PPN-**4**. The correct formulation of this material is $PPN[CpCoNO]\cdot(CH_3CN)_x$, where x was determined to be about 0.6 by integration of the Cp vs. CH_3CN resonances in the ^1H NMR spectrum, and was confirmed by elemental analysis: IR (CH_3CN) 1580 (s) cm^{-1}; ^1H NMR (Me_2SO-d_6) δ 7.55 (m, 30 H), 14.1 (s, 5 H), 2.06 (s, 0.8 H, CH_3CN). Anal. Calcd for $C_{42.2}H_{36.8}N_{2.6}OP_2Co$: C, 70.66; H, 5.17; N, 5.08. Found: C, 70.31; H, 5.44; N, 4.91.

In a similar manner, 0.30 g (1.69 mmol) of Na[MeCpCoNO] was treated with 0.468 g (0.847 mmol) of PPNCl in 10 mL of THF to yield 0.50 g of complex $PPN[MeCpCoNO]\cdot(CH_3CN)$, where the 1:1 stoichiometry of the solvent in the PPN salt was confirmed by ^1H NMR spectroscopy and elemental analysis: IR (CH_3CN) 1580 cm^{-1}; ^1H NMR (Me_2SO-d_6) δ 7.50 (m, 30 H), 3.9 (m, 4 H), 2.13 (s, 3 H), 2.06 (s, 3 H, CH_3CN). Anal. Calcd for $C_{44}H_{40}N_3OP_2Co$: C, 70.68; H, 5.39; N, 5.62. Found: C, 70.82; H, 5.42; N, 5.53.

CpCo(CH_3NO)PPh_3 (6a). In the drybox, a 100-mL round-bottom flask fitted with a magnetic stir bar was charged with 200 mg (1.13 mmol) of **4**, 300 mg (1.15 mmol) of PPh_3, and 50 mL of THF. With

(17) Hoyano, J. K.; Legzdins, P.; Malito, J. T. *J. Chem. Soc., Dalton Trans.* **1975**, 1022–1025.
(18) Theopold, K. H. Ph.D. Thesis, University of California, Berkeley, 1982.
(19) Casey, C. P.; Jones, W. D.; Harsey, G. S. *J. Organomet. Chem.* **1981**, *206*, C38–39.
(20) Chaudhari, F. M.; Knox, G. R.; Pauson, P. L. *J. Chem. Soc. C* **1967**, 2255–2260.
(21) King, R. B. *Inorg. Chem.* **1968**, *7*, 90–94.
(22) Rausch, M. D.; Genetti, R. A. *J. Org. Chem.* **1970**, *35*, 3888–3897.

stirring, 72 μL (164 mg, 1.15 mmol) of CH_3I was added. Immediately the solution changed color from violet to blue and then became dark green after 10 min. The solution was allowed to stir for 1 h, after which the THF was removed by vacuum transfer, leaving a dark green residue. In the drybox, the residue was taken up in a minimum of benzene and filtered through a 30-mL fine frit. After the benzene was removed by vacuum transfer, the remaining green oil was recrystallized from 2/1 pentane/toluene at −40 °C. The dark microcrystals collected were washed with hexanes and then suction dried to yield 410 mg (0.928 mmol, 81% yield) of **6a**: mp 115 °C dec; IR (THF) 1485 (w), 1435 (m), 1305 (s) cm^{-1}; ^1H NMR (C_6D_6) δ 7.65 (m, 6 H), 7.0 (m), 4.5 (s, 5 H), 2.6 (d, 3 H, J = 3 Hz). Anal. Calcd for $C_{24}H_{23}NOPCo$; C, 66.82; H, 5.83; N, 3.24. Found: C, 66.94; H, 5.45; N, 3.30.

$CpCo(CH_3CH_2NO)PPh_3$ (6b). Following the identical procedure outlined above for the synthesis and purification of **6a**, 200 mg (1.13 mmol) of **4**, 300 mg (1.15 mmol) of PPh_3, and 90 μL (176 mg, 1.13 mmol) of CH_3CH_2I were mixed in 50 mL of THF to yield 114 mg (0.257 mmol) of **6b**: 23% yield; mp 125 °C dec; IR (THF) 1485 (w), 1435 (m), 1300 (w), 1230 (m) cm^{-1}; ^1H NMR (C_6D_6) δ 7.65 (m, 6 H), 7.0 (m), 4.5 (s, 5 H), 3.2 (m, J = 1.5 Hz, 2 H), 1.15 (t, 3 H, J = 7 Hz). Anal. Calcd for $C_{25}H_{25}NOPCo$: C, 67.56; H, 5.63; N, 3.15. Found: C, 67.62; H, 5.80; N, 3.09.

$CpCo[(CH_3)_2CHNO]PPh_3$ (6c). Following the identical procedure described above, in a 100-mL round-bottom flask fitted with a magnetic stir bar, 1.0 g (5.65 mmol) of **4**, 0.464 g (1.77 mmol) of PPh_3, and 1.44 g (8.47 mmol) of isopropyl iodide in 50 mL of THF gave 210 mg (0.457 mmol) of **6c**: 26% yield; mp 121–123 °C; IR (THF) 1430 (w), 1370 (w), 1350 (w); ^1H NMR (THF-d_8) δ 7.61 (m, 6 H), 7.30 (m, 9 H), 4.94 (quint, 1 H, J = 6.4 Hz), 0.89 (d, 6 H, J = 6.5 Hz). Anal. Calcd for $C_{26}H_{27}NOPCo$: C, 67.97; H, 5.94; N, 3.05. Found: C, 67.97; H, 5.83; N, 2.93.

$CpCo(p\text{-}CH_3C_6H_4CH_2NO)PPh_3$ (6d). In the drybox, a round-bottom flask containing a magnetic stir bar was charged with 0.50 g (2.82 mmol) of **4** in 30 mL of THF. With stirring, 0.52 g (2.82 mmol) of *p*-methylbenzyl bromide was added, and the red solution immediately turned green. After 1 min, 0.741 g (2.82 mmol) of PPh_3 was added to the reaction mixture, and the solution was allowed to stir for 8 h. The solvent was removed by vacuum transfer to yield a green oil, which was taken up in a minimum of CH_2Cl_2. Enough pentane was added to the resulting solution to precipitate the NaBr, which was removed by filtration through a fine fritted funnel. After the solvent was removed by vacuum transfer, the oily green residue obtained from the filtered solution was recrystallized from 3/1 pentane/CH_2Cl_2 at −40 °C to give 0.256 g (0.422 mmol, 15% yield) of product. Elemental analysis and ^1H NMR spectroscopy show the correct formulation of this material to be **6d**·CH_2Cl_2: mp 72–76 °C; IR (THF) 1340 (w), 1305 (w) cm^{-1}; ^1H NMR (CD_3CN) δ 7.53–7.15 (m, 19 H), 5.44 (s, 2 H, CH_2Cl_2), 4.53 (s, 5 H), 4.28 (s, 2 H), 2.34 (s, 3 H). Anal. Calcd for $C_{32}H_{29}Cl_2NOPCo$: C, 63.37; H, 5.16; N, 2.31. Found: C, 62.99; H, 5.19; N, 2.28.

Reaction of 6d with $LiAlH_4$. In the drybox, a 200-mL round-bottom flask containing an efficient stir bar was charged with 0.247 g (0.407 mmol) of **4** in 70 mL of Et_2O and fitted with a pressure equalizing addition funnel and a reflux condenser. The addition funnel was charged with 0.160 g (0.422 mmol) of $LiAlH_4$ in 10 mL of Et_2O and stoppered with a serum cap, as was the remaining open neck of the flask. The assembly was removed from the drybox and maintained under a positive flow of argon through a syringe needle inserted into the dropping funnel and extending into the $LiAlH_4/Et_2O$ slurry. In this manner, the bubbling argon kept the slurry dispersed. After the flask was cooled in a 0 °C bath, the $LiAlH_4$ was added with stirring over the course of 10 min. The reaction solution was allowed to stir at room temperature for 2 h, and then the excess $LiAlH_4$ was quenched by recooling the solution to 0 °C and adding successively 0.16 mL of H_2O, 0.16 mL of 15% NaOH, and 0.430 mL of H_2O.[23] The reaction was removed from the argon source and allowed to stir for 2 h at room temperature after the addition of 100 mL of Et_2O. The solution was then filtered through a 150-mL medium frit and the solvent removed by vacuum transfer. The oily residue obtained was redissolved in a minimum of Et_2O, and 0.1 mL of concentrated HCl was added. The white precipitate which formed was filtered onto a 15-mL medium frit, washed with THF, and recrystallized from 3/1 CH_3OH/Et_2O at 0 °C to give 0.059 g (0.374 mmol, 92% yield) of *p*-methylbenzylamine hydrochloride, pure by ^1H NMR spectroscopy. The product was identified on the basis of its ^1H NMR and IR spectra, which were identical with those of an authentic sample, prepared by the reaction of HCl with *p*-methylbenzylamine (Aldrich) in ether: IR (KBr) 3000 (s, br), 1610 (m), 1595 (m), 1520 (s), 1380 (m), 1205 (m), 1210 (m), 810 (m), 550 (m) cm^{-1}; ^1H NMR (Me_2SO-d_6) δ 8.45 (s, 3 H), 7.38–7.18 (m, 4 H), 3.93 (m, 2 H), 2.29 (s, 3 H).

Reaction of 4 with CH_3CD_2I. An NMR tube with a ground glass joint was charged in the drybox with 20.0 mg (0.113 mmol) of **4**, 30.0 mg (0.114 mmol) of PPh_3, and 11.0 mg (0.059 mmol) of ferrocene as an internal standard. The NMR tube was then fitted with a vacuum stopcock and attached to a vacuum line, where 1.0 mL of THF-d_8 was vacuum transferred into the tube. With use of a known volume bulb, 17.0 mg (0.107 mmol) of the iodide was condensed into the NMR tube, after which the tube was sealed under vacuum at −196 °C. The sealed tube was then placed in the probe of an NMR spectrometer maintained at 0 °C. The smooth formation of α-deuterated ethylnitroso complex was observed without scrambling of protons into the α position (δ 3.49): ^1H NMR (THF-d_8) δ 7.6 (m, 6 H), 7.3 (m, 9 H), 4.78 (s, 5 H), 4.08 (Cp_2Fe), 1.05 (s, br, 3 H).

Double-Labeling Crossover Experiment. In the drybox, 20.0 mg (0.113 mmol) of **4** and 30.0 mg (0.114 mmol) of PPh_3 were added to a 10-mL pear-shaped flask equipped with magnetic stir bar. A second flask was charged with 27.0 mg (0.141 mmol) of Na[MeCpCoNO] and 30.0 mg (0.114 mmol) of PPh_3. Two 1-mL volumetric flasks were also prepared, one containing 8 μL of CH_3I in 0.7 mL of THF-d_8 and the other 8 μL of $^{13}CH_3I$ in 0.7 mL of THF-d_8. These items were carefully stoppered with securely fitting serum caps, removed from the drybox, and cooled to −78 °C (CO_2/2-propanol) under a flow of nitrogen. In addition, a jointed NMR tube was fitted with a small Claisen distilling head, having one opening topped with a vacuum stopcock and the other stoppered with a serum cap. The entire assembly was kept under a flow of nitrogen and cooled to −196 °C. With use of a stainless-steel cannula, the CH_3I and $^{13}CH_3I$ solutions were introduced to the flasks containing **4** and Na[MeCpCoNO], respectively. The two deep blue solutions were allowed to stir for 2 min, after which the contents of the flask originally containing **4** were transferred via cannula into the other pear-shaped flask. The combined solution containing **5a** and $MeCpCo(^{13}CH_3)(NO)$ was allowed to stir for 10 min before transferring the contents of the flask by cannula to the precooled NMR tube. The tube was then sealed under vacuum at −196 °C. The tube was warmed to −78 °C and placed in the probe of an NMR spectrometer maintained at −50 °C. Analysis of the $^{13}C\{^1H\}$ NMR spectrum of the reaction solution at this temperature (20 acquisitions) revealed ^{13}C enrichment only at the resonance of the cobalt-bound methyl group of $MeCpCo(^{13}CH_3)(NO)$ (δ −10.25). No resonance for the cobalt-bound methyl group of **5a** (δ −16.01) was observed. The tube was then allowed to warm to 25 °C to allow the insertion reaction to take place. After 40 min, the $^{13}C\{^1H\}$ NMR spectrum (100 acquisitions) showed a prominent resonance of the nitrosomethane ligand of $CpCo(^{13}CH_3NO)PPh_3$ at δ 76.0, with no significant ^{13}C enrichment (above 10%) of the nitrosomethane ligand of **6a** at δ 76.7.

Kinetic Measurements by UV/vis Spectroscopy. Stock solutions containing known concentrations of PPh_3 in THF were freshly prepared in the drybox before each run. Known amounts of **4** were added to an aliquot of measured volume of the phosphine stock solution to create stock reaction solutions of **4** and PPh_3. The sample and reference cuvettes were then filled in the drybox with the reaction solution and the PPh_3 solutions respectively (the sample cuvette was fitted with a small stir bar). Both cuvettes were stoppered securely with serum caps and removed from the drybox. In preparation for each kinetic run listed in Table I, 3 μL of carefully degassed CH_3I was extracted under a flow of argon from a serum-stoppered flask with a syringe. The CH_3I was added quickly to the cuvette containing the **4**/PPh_3 solution and was allowed to stir for 15 s, assuring the complete formation of **5a**. The cuvette was then placed in the spectrophotometer, and data collection was started. During the course of the reaction, the temperature was maintained at 18.0 ± 0.5 °C. The system capabilities allowed complete scans of the UV/vis spectrum to be completed in 1 s. For the initial half-life of the reaction, scans were collected every 5 s. The change of absorbance at λ 415 nm was used to determine the course of the reaction, and from this information[24] the value of k_{obsd} for a given [PPh_3] can be derived according to eq 9.

$$\ln (A_\infty - A_t) = -k_{obsd}t + \ln (A_\infty - A_0) \quad (9)$$

Kinetic Measurements by ^1H NMR Spectroscopy. All samples for the kinetic runs listed in Table II were prepared in the manner described below.

A jointed NMR tube was charged in the drybox with the appropriate amounts of **4**, PEt_3, internal standard ferrocene, and a known volume of THF-d_8. Using a syringe, a known volume of CH_3I was added to a small flask, which was then fitted with a vacuum stopcock and attached to the NMR tube via a vacuum transfer arm. The entire assembly was topped with a stopcock and evacuated on a vacuum line. The CH_3I was vacuum transferred onto the frozen reaction solution, and the NMR tube was

(23) Becker, P. N.; White, M. A.; Bergman, R. G. *J. Am. Chem. Soc.* **1980**, *102*, 5676–5677.

(24) Moore, J. W.; Pearson, R. G. "Kinetics and Mechanism"; Wiley: New York, 1981.

sealed at −196 °C. In preparation for each run, the tube was warmed to −78 °C in a CO_2/2-propanol bath with shaking to assure the complete formation of **5a**. The tube was then warmed to room temperature and placed in the probe of an NMR spectrometer maintained at 28.0 ± 0.5 °C. Data sets were collected over 3 half-lives of the reaction. A typical data set consisted of 12 acquisitions at 201.947 MHz with a SW = ±1113.58 Hz, a pulse width of 20°, and a 5-s delay between pulses. The progress of the reaction was monitored by integrating the Cp resonances of **5a** and **6e** at δ 5.4 and 5.15, respectively, vs. the ferrocene resonance at δ 4.1.

Acknowledgment. We are grateful for support of this work from National Institutes of Health, Grant No. GM-25459. We also wish to thank Dr. Peter Hoffmann for providing us with the results of his calculations prior to publication. R.G.B. acknowledges a Research Professorship from the Miller Institute for Basic Research in Science at U. C. Berkeley, 1982–1983.

Registry No. 3, 51862-20-5; **4**, 78305-62-1; **5a**, 78305-63-2; **6a**, 78305-64-3; **6b**, 78305-65-4; **6c**, 85454-60-0; **6d**, 85454-61-1; **6e**, 85454-62-2; **8a**, 85454-63-3; CH_3I, 74-88-4; CH_3CH_2I, 75-03-6; PPh_3, 603-35-0; PEt_3, 554-70-1; $(\eta^5\text{-}MeC_5H_4)Co(CO)_2$, 75297-02-8; $CH_3C_5H_5$, 26519-91-5; $Co_2(CO)_8$, 10210-68-1; $CpCo(CO)_2$, 12078-25-0; NO, 10102-43-9; $[MeCpCo(NO)]_2$, 85454-64-4; Na[MeCpCoNO], 85454-65-5; PPNCl, 21050-13-5; PPN-**4**, 85454-66-6; PPN[MeCpCoNO], 85454-68-8; $LiAlH_4$, 16853-85-3; methyl *p*-toluenesulfonate, 80-48-8; isopropyl iodide, 75-30-9; *p*-methylbenzyl bromide, 104-81-4; Co, 7440-48-4.

Activation of C–H Bonds in Saturated Hydrocarbons on Photolysis of $(\eta^5\text{-}C_5Me_5)(PMe_3)IrH_2$. Relative Rates of Reaction of the Intermediate with Different Types of C–H Bonds and Functionalization of the Metal-Bound Alkyl Groups

Andrew H. Janowicz and Robert G. Bergman*

Contribution from the Department of Chemistry, University of California, and Materials and Molecular Research Division, Lawrence Berkeley Laboratory, Berkeley, California 94720.
Received October 20, 1982

Abstract: The full details of experiments on a homogeneous system which successfully converts completely saturated alkanes into hydridoalkylmetal complexes (M + RH → R–M–H) are reported. Irradiation of $(\eta^5\text{-}C_5Me_5)(PMe_3)IrH_2$ (**5**) in saturated hydrocarbons (R–H) using a 500-W Oriel focused-beam mercury lamp leads to extrusion of H_2 and production of the hydrido alkyl complexes $(\eta^5\text{-}C_5Me_5)(PMe_3)Ir(R)(H)$. Competition experiments have allowed measurement of the relative rates at which the intermediate formed on H_2 loss (presumably the coordinatively unsaturated complex $(\eta^5\text{-}C_5Me_5)(PMe_3)Ir$) reacts with different types of C–H bonds. Relative to cyclohexane (1.0), these are as follows: benzene (4.0), cyclopropane (2.65), cyclopentane (1.6), neopentane (1.14), cyclodecane (0.23), and cyclooctane (0.09). Reductive elimination of hydrocarbon occurs at elevated temperature, regenerating $(\eta^5\text{-}C_5Me_5)(PMe_3)Ir$, which may then react with another hydrocarbon acting as solvent; thus the C–H activation process can also be induced thermally. C–H bonds having high bond energies react relatively rapidly; this fact, along with crossover experiments, suggests that radical intermediates are not involved in the C–H activation reaction. Treatment of the hydrido neopentyl complex **8** with $CHBr_3$ converts it to the corresponding bromo neopentyl complex **10**. This material reacts with $HgCl_2$ to give neopentylmercuric chloride, which forms neopentyl bromide on reaction with Br_2. Thus overall stoichiometric conversion of hydrocarbons to functionalized organic molecules is feasible in this system. The factors which have been presumed to influence the rates of reaction of transition-metal complexes with saturated C–H bonds–notably the need for electron-rich metals and close proximity of reacting centers—are discussed in detail.

One of the most intriguing—and yet elusive—goals of organometallic chemistry has been the use of transition-metal complexes to "activate" carbon–hydrogen bonds in completely saturated organic compounds.[1] One impetus for research in this area is that saturated hydrocarbons are among the most ubiquitous, and chemically stable, of all organic materials, due to the high values of their C–H and C–C bond energies. It is important to learn the chemical requirements for causing such stable substances to react and, if such reactions are found, to understand their mechanisms. On a more practical level, understanding C–H activation should help to develop methods for converting saturated hydrocarbons, such as those found in petroleum and formed in Fischer–Tropsch reactions, into functionalized compounds more easily utilized in chemical conversions.

Scheme I

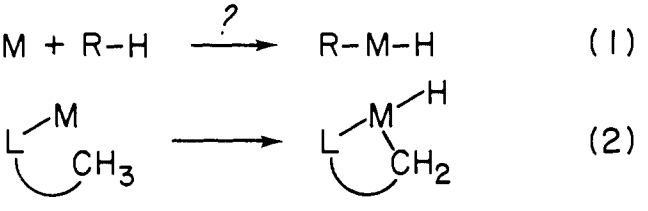

Saturated hydrocarbons are of course not completely unreactive, and as a result they have a long history of activation by nonmetallic reagents and methods. Hydrocarbon thermal reactions and combustion have been studied by both chemists and chemical engineers, and there are well-known free radical reactions (e.g.,

(1) (a) Parshall, G. W. *Catalysis (London)* **1977**, *1*, 335. (b) Shilov, A. E.; Shteinman, A. A. *Coord. Chem. Rev.* **1977**, *24*, 97. (c) Webster, D. E. *Adv. Organomet. Chem.* **1977**, *15*, 147. (d) Parshall, G. W. "Homogeneous Catalysis"; Wiley-Interscience: New York, 1980; p 179 ff. (e) Collman, J. P.; Hegedus, L. S. "Principles and Applications of Organotransition Metal Chemistry"; University Science Books: Mill Valley, CA, 1980, p 222 ff. (f) Halpern, J. *Discuss. Faraday Soc.* **1968**, *46*, 7.

0002-7863/83/1505-3929$01.50/0